Bas champs : the come-back

Angéline Nemeth

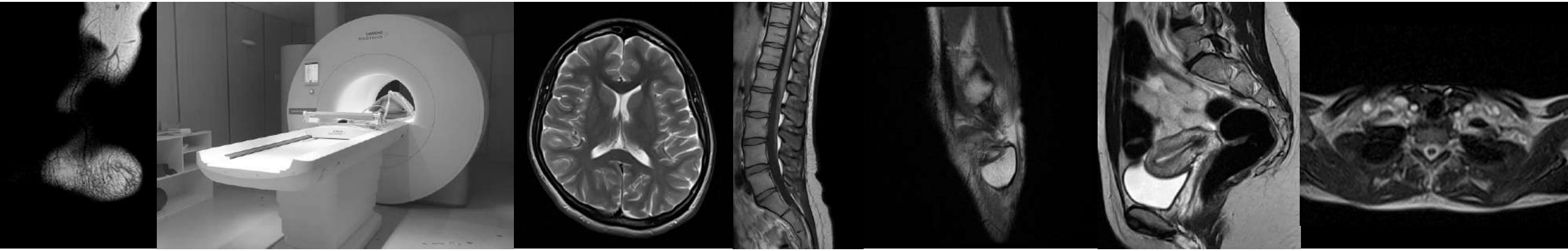

The come-back

- Improvements in hardware :
  - closed Helium-free magnets,
  - RF receiver systems
  - faster gradients
  - flexible sampling schemes including parallel imaging and compressed sensing
  - use of AI at all stages of the imaging process

RESULTS BY YEAR 733 publications en 2025

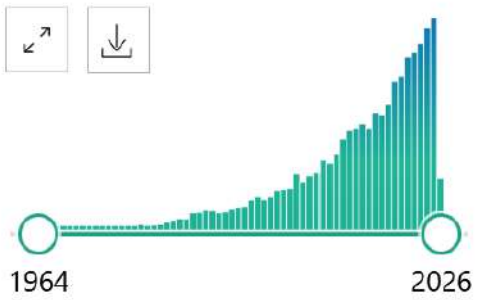

Nombre de résultats Pubmed avec les mots clés « low field MRI »

46 publications en 2025

RESULTS BY YEAR

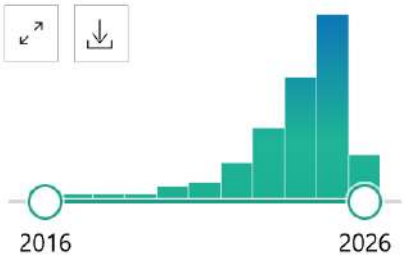

Nombre de résultats Pubmed avec les mots clés « 0.55T MRI »

=> have made low-field MRI a clinically viable supplement to conventional MRI

Le come-back

[Campbell-Washburn, A. E.; et al. Opportunities in Interventional and Diagnostic Imaging by Using High-Performance Low-Field-Strength MRI. Radiology 2019, 293 (2), 384–393. https://doi.org/10.1148/radiol.2019190452.]

- Un système d'IRM commercial de **1,5 T => 0,55 T** tout en conservant un matériel haute performance et des gradients blindés (45 mT/m ; 200 T/m/sec) :
  - Aux interfaces air-tissue :

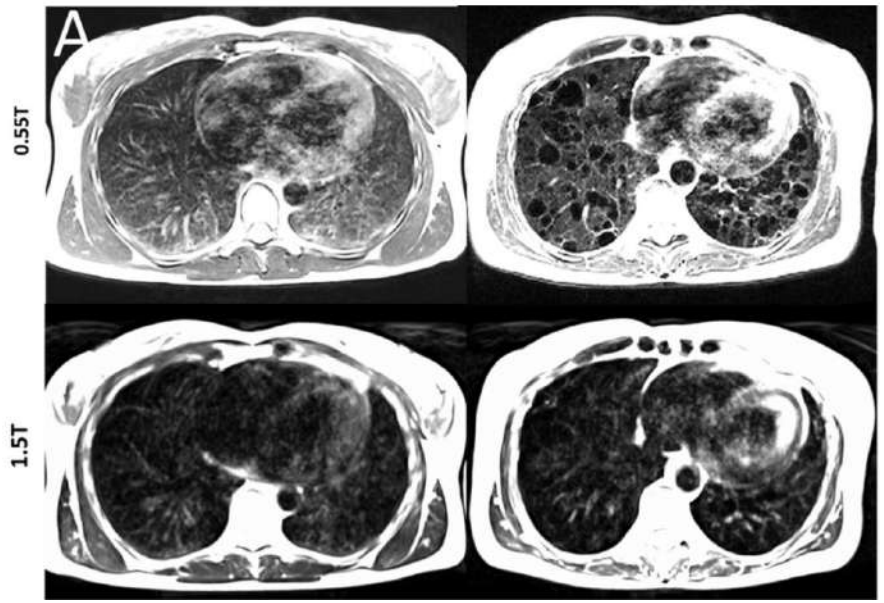

A, Lungs show increased signal intensity at 0.55 T compared with 1.5 T because of improved field homogeneity demonstrated in a healthy 26-year-old woman and a 54-year-old woman with lymphangioleiomyomatosis (T2-weighted fast spin echo; repetition time msec/echo time msec, 4403/47; field of view, 270 3 360 mm; 480 3 640; 32 sections; section thickness, 6 mm; bandwidth, 260 Hz per pixel; respiratory triggered).

Real time speech imaging at 0.55T with 11.3 msec temporal resolution. Clear delineation of the tissue is observed because of reduced distortion at this low field strength.

Le come-back

Table 1: Tissue Relaxation Parameters at 0.55 T versus Reference 1.5-T Values

Tissue	T1 (msec)	T2 (msec)	T2* (msec)	T2*-to-T2 Ratio (%)
White matter				
0.55 T	493 ± 33	89 ± 9	72 ± 12	81
1.5 T	608–884	54–96	48–60	72
Gray matter				
0.55 T	717 ± 82	112 ± 7	86 ± 9	77
1.5 T	1002–1304	93–109	67–79	72
Myocardium				
0.55 T	701 ± 24	58 ± 6	47 ± 4	80
1.5 T	950–1030	40–58	30–37	68
Arterial blood				
0.55 T	1122 ± 85	263 ± 27	...	...
1.5 T	1441–1898	254–290	...	...
Liver				
0.55 T	339 ± 31	66 ± 6	43 ± 4	65
1.5 T	576–586	46–55	26–33	59
Lung				
0.55 T	971 ± 62	61 ± 11	10 ± 2	17
1.5 T	1171–1333	41	1–2	5
Kidney cortex				
0.55 T	651 ± 48	101 ± 7	82 ± 17	82
1.5 T	690–966	55–87	49–51	70
Fat				
0.55 T	187 ± 10	93 ± 16	...	...
1.5 T	288–343	53–84	...	...

Note.—The 0.55-T values are means ± standard deviation; the 1.5-T values are ranges. Imaging sequence parameters and 1.5T reference list are provided in Appendix E1 Materials section (online). T2*-to-T2 ratio was calculated from mean values. For 0.55 T, participants were as follows: white/gray matter, nine participants (mean age, 31 years ± 12; six women); myocardium/blood/lung, 22 participants (mean age, 35 years ± 12; six women); and liver/kidney/fat, seven participants (mean age, 23 years ± 4; five women).

[Campbell-Washburn, A. E.; et al. Opportunities in Interventional and Diagnostic Imaging by Using High-Performance Low-Field-Strength MRI. Radiology 2019, 293 (2), 384–393. https://doi.org/10.1148/radiol.2019190452.]

Le come-back

[Campbell-Washburn, A. E.; et al. Opportunities in Interventional and Diagnostic Imaging by Using High-Performance Low-Field-Strength MRI. Radiology 2019, 293 (2), 384–393. https://doi.org/10.1148/radiol.2019190452.]

- A bas-champ => repenser les séquences d'acquisition :

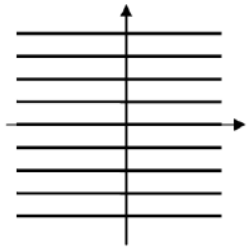

Cartésien

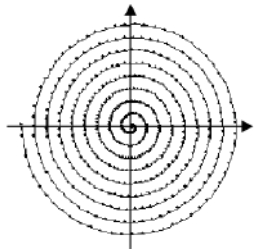

Spiral

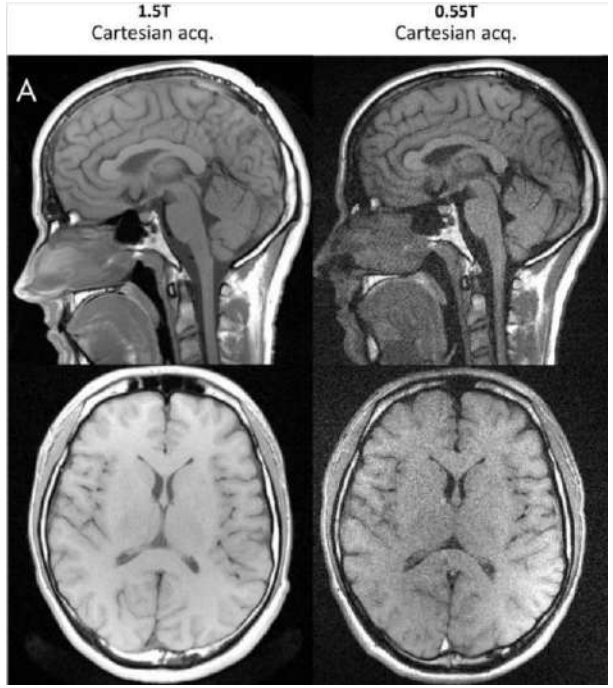

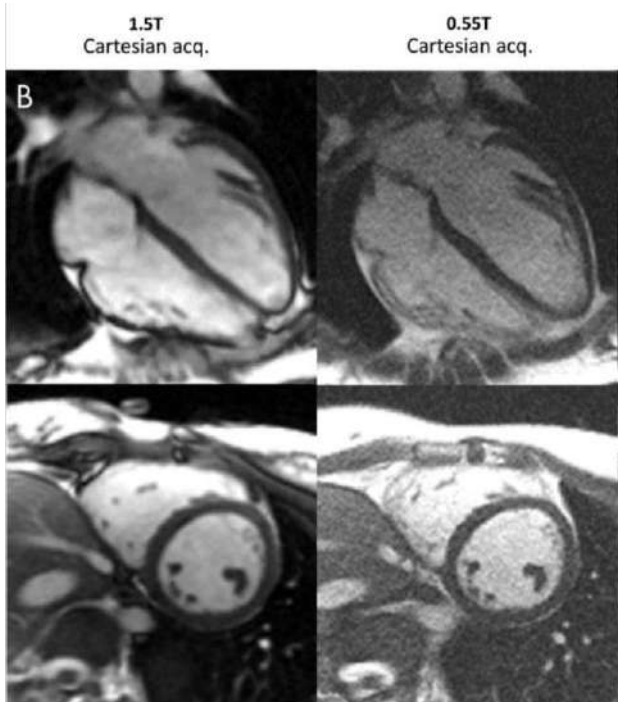

Le come-back

- Opportunités :
  - Avoir une ouverture plus large => étudier des populations difficilement accessible à champs standard
    - Surpoids et obésité
    - Femme enceinte

Composition du corps à 0,55T

[Nayak, K. S.; et al. , A. Body Composition Profiling at 0.55T: Feasibility and Precision. Magn. Reson. Med. 2023, 90 (3), 1114–1120. https://doi.org/10.1002/mrm.29682.

Mesure :

- volumes de tissus adipeux (viscéral vs sous-cu
- volumes des muscles
- contenu lipidique (PDFF)

Graisse Eau

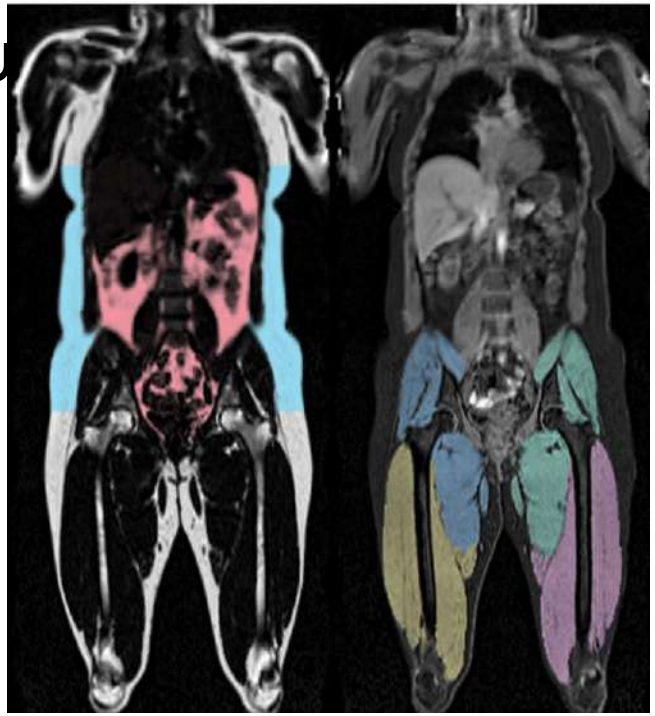

Imagerie du fétus à 0,55T

- Intérêt médical: diagnostic des anomalies du **fétus** et du **placenta.**

- Les artefacts fréquemment rencontrés à champ standard et réduit à bas-champ :
  - distorsions géométriques dues aux interfaces air-tissu à proximité des intestins maternels
  - artefacts B1 liés à la conductivité élevée du liquide amniotique

- Opportunités d'un champ 0,55T avec une plus large ouverture :
  - étudier des patientes obèses une population présentant un risque accru de complications de grossesse telles que la prééclampsie et le diabète gestationnel, et chez laquelle une évaluation précise est donc essentielle.

Imagerie du fétus à 0,55T

[Verdera et al. Characterizing T1 in the fetal brain and placenta over gestational age at 0.55T. MagnResonMed. 2024 November 01; 92(5): 2101–2111. doi:10.1002/mrm.30193.]

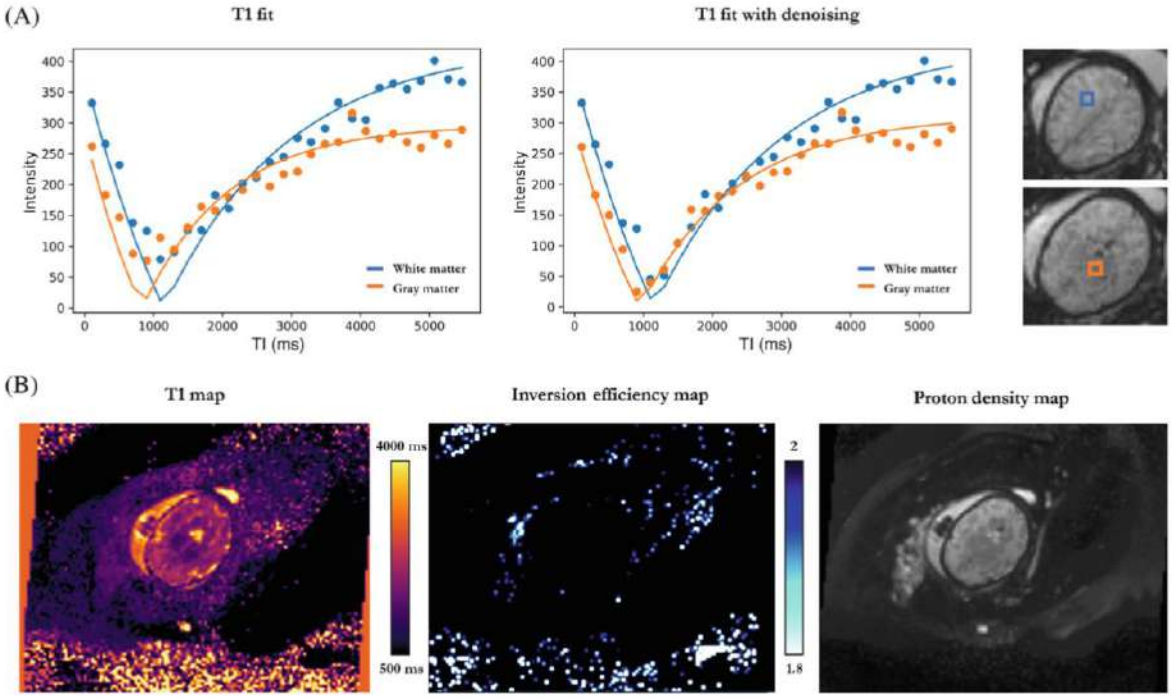

Figure 4. T1 fetal brain results for a subject at 32 + 6 weeks GA.
(A) Individual data points across inversion time and their corresponding T1 fits for hemispheric white matter (blue) and deep grey matter (orange), without and with the denoising step. Selected voxels are shown in a colored box next to the plots. (B) Axial view of the whole image T1, inversion efficiency and proton density maps, from left to right.

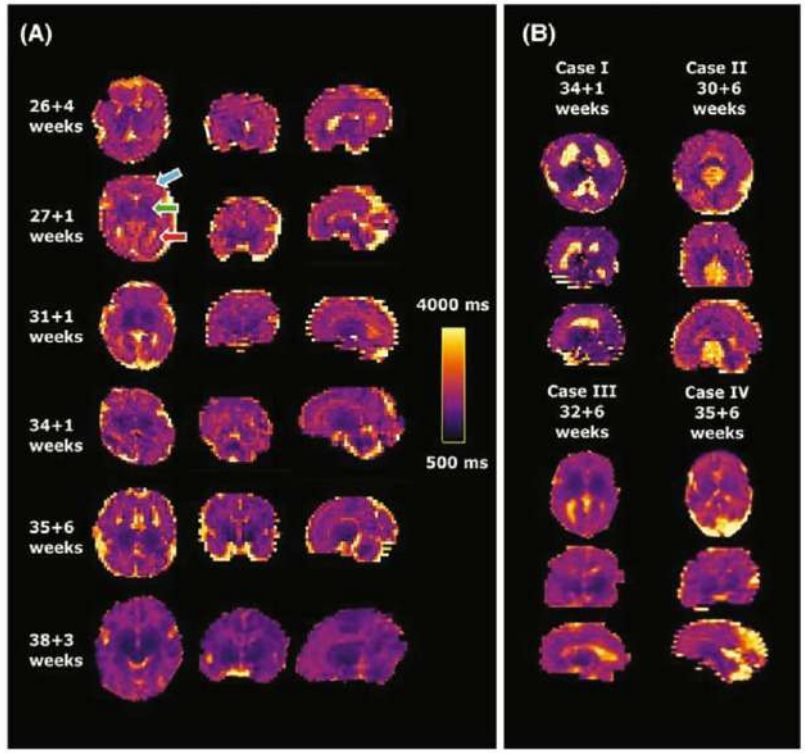

Figure 5.
Obtained high-resolution brain T1 maps in axial, coronal and sagittal orientation from (A) six control fetuses sorted by gestational age and (B) four clinical examples with ventriculomegaly, mid-line brain cyst, unilateral ventriculomegaly and enlarged cisterna magna from left to right and top to bottom are shown. The same scaling is used for all cases as indicated in (A). Most cases were acquired axial to the fetal brain, these acquired in tilted orientations were rotated to true radiological planes. Blue arrow points at white matter, green arrow to deep grey matter and red arrow to ventricles.

Imagerie du fétus à 0,55T

[Slator, P. J.; Verdera, J. A.; et al., J. Low-Field Combined Diffusion-Relaxation MRI for Mapping Placenta Structure and Function. https://doi.org/10.1101/2023.06.06.23290983]

[Ponrartana, S.; et al. Low-Field 0.55 T MRI Evaluation of the Fetus. Pediatr. Radiol. 2023, 53 (7), 1469–1475. https://doi.org/10.1007/s00247-023-05604-x.]

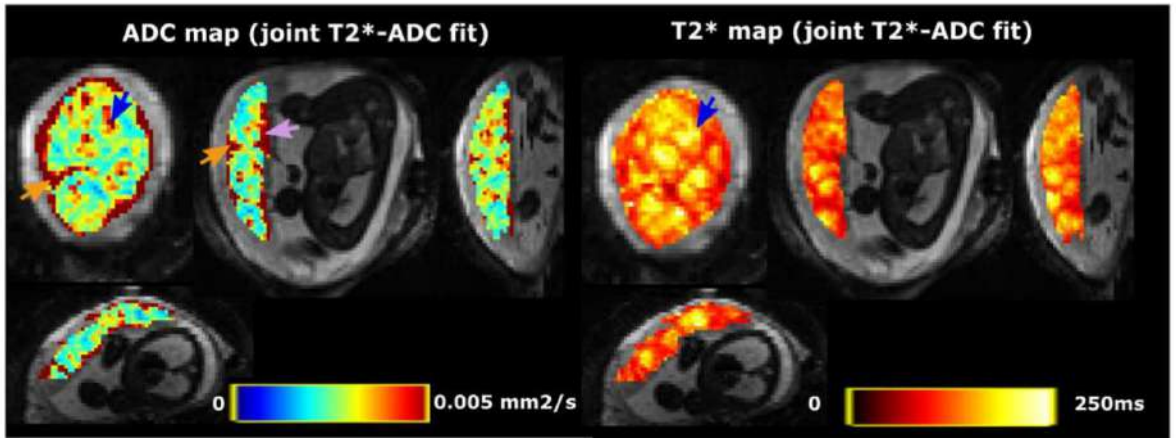

Figure 2: Detailed view into one example dataset (control, GA = 27.14 weeks - same participant as Figure 1). Top row: the ADC and T2* map from the joint fit. Bottom row: the T2* map from the additional multi-echo gradient echo scan. The blue arrow shows the increased ADC and T2* in the lobule centres, the pink arrow the increase on the chorionic plate and the orange arrows the increase in ADC and reduction in T2* in the septa between the lobules.

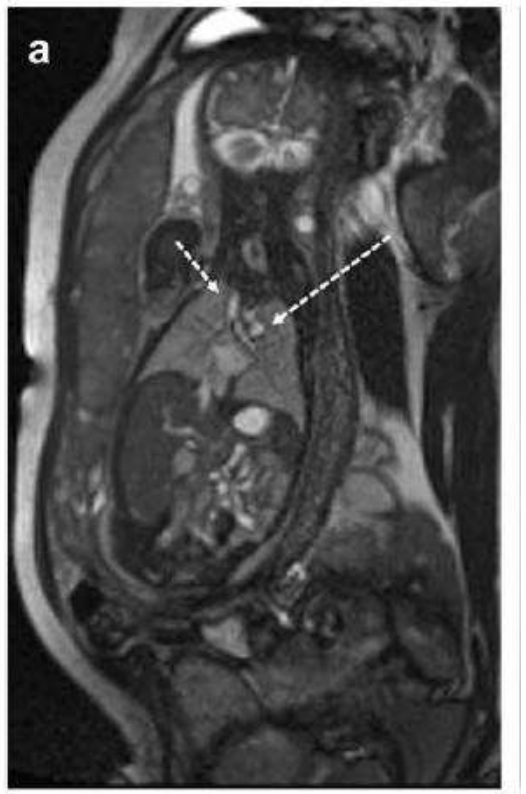

Fig. 2 32-week gestational age fetus. Coronal balanced steady-state free precession (bSSFP) (**a**) and half-Fourier single-shot turbo spin echo (HASTE) (**b**) images show a normal fluid-filled tracheo-

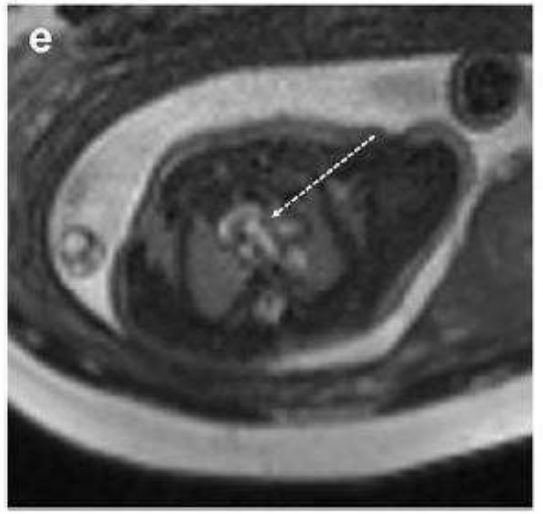

Le come-back

- Opportunités :
  - Avoir une ouverture plus large => étudier des populations difficilement accessible à champs standard
    - Surpoids et obésité
    - Femme enceinte
  - Moins d'artéfact de susceptibilité magnétique
    - Imagerie des prothèses

Prothèse de hanche

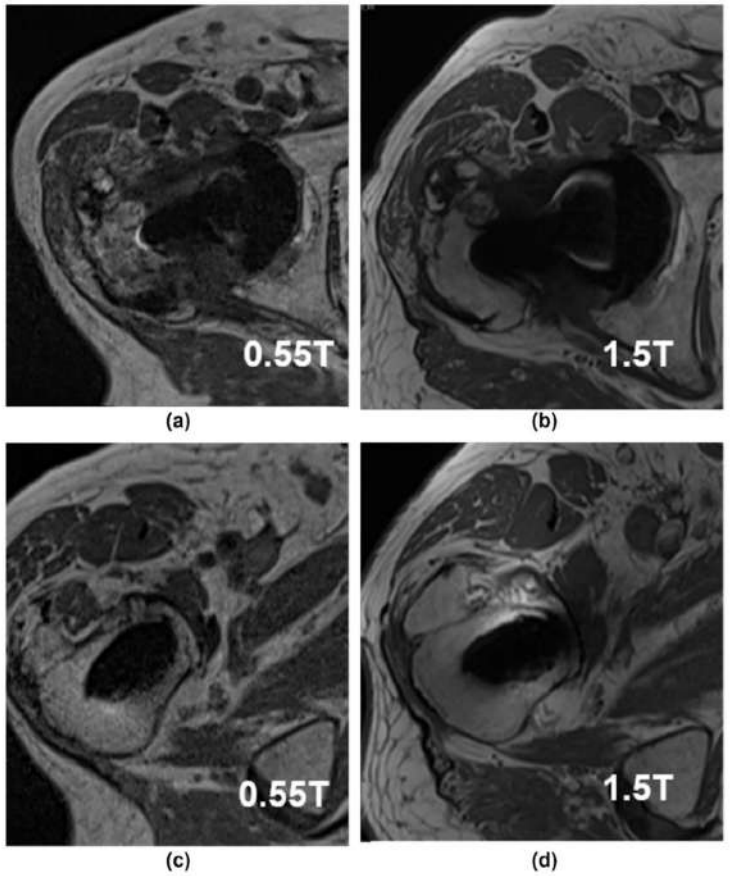

Figure 2 Comparison of artifacts at the level of the acetabulum (a),(b) and proximal stem (c),(d) at 0.55T (a),(c) and 1.5T (b),(d) in T1 weighting.

[Breit et al. New-Generation 0.55T MRI in Patients with Total Hip Arthroplasty: A Comparison with 1.5T MRI. Clin. Radiol. 2025, 81, 106758. https://doi.org/10.1016/j.crad.2024.106758]

Biblio

- Campbell-Washburn, A. E.; Ramasawmy, R.; Restivo, M. C.; Bhattacharya, I.; Basar, B.; Herzka, D. A.; Hansen, M. S.; Rogers, T.; Bandettini, W. P.; McGuirt, D. R.; Mancini, C.; Grodzki, D.; Schneider, R.; Majeed, W.; Bhat, H.; Xue, H.; Moss, J.; Malayeri, A. A.; Jones, E. C.; Koretsky, A. P.; Kellman, P.; Chen, M. Y.; Lederman, R. J.; Balaban, R. S. Opportunities in Interventional and Diagnostic Imaging by Using High-Performance Low-Field-Strength MRI. *Radiology* **2019**, *293* (2), 384–393. https://doi.org/10.1148/radiol.2019190452.

- Nayak, K. S.; Cui, S. X.; Tasdelen, B.; Yagiz, E.; Weston, S.; Zhong, X.; Ahlgren, A. Body Composition Profiling at 0.55T: Feasibility and Precision. *Magn. Reson. Med.* **2023**, *90* (3), 1114–1120. https://doi.org/10.1002/mrm.29682.

- Verdera, J. A.; Tomi-Tricot, R.; Story, L.; Rutherford, M. A.; Ourselin, S.; Hajnal, J. V.; Malik, S. J.; Hutter, J. Characterizing T1 in the Fetal Brain and Placenta over Gestational Age at 0.55T. *Magn. Reson. Med.* **2024**, *92* (5), 2101–2111. https://doi.org/10.1002/mrm.30193.

- Slator, P. J.; Verdera, J. A.; Tomi-Tricot, R.; Hajnal, J. V.; Alexander, D. C.; Hutter, J. Low-Field Combined Diffusion-Relaxation MRI for Mapping Placenta Structure and Function. *medRxiv* **2023**, 2023.06.06.23290983. https://doi.org/10.1101/2023.06.06.23290983.

- Ponrartana, S.; Nguyen, H. N.; Cui, S. X.; Tian, Y.; Kumar, P.; Wood, J. C.; Nayak, K. S. Low-Field 0.55 T MRI Evaluation of the Fetus. *Pediatr. Radiol.* **2023**, *53* (7), 1469–1475. https://doi.org/10.1007/s00247-023-05604-x.